Magnetic Suspension Array Technology: Controlled Synthesis and Screening in Microfluidic Networks

Gungun Lin, Dmitriy D. Karnaushenko, Gilbert Santiago Cañón Bermúdez, Oliver G. Schmidt, and Denys Makarov**

Information tagging and processing are vital in information-intensive applications, e.g., telecommunication and high-throughput drug screening. Magnetic suspension array technology may offer intrinsic advantages to screening applications by enabling high distinguishability, the ease of code generation, and the feasibility of fast code readout, though the practical applicability of magnetic suspension array technology remains hampered by the lack of quality administration of encoded microcarriers. Here, a logic-controlled microfluidic system enabling controlled synthesis of magnetic suspension arrays in multiphase flow networks is realized. The smart and compact system offers a practical solution for the quality administration and screening of encoded magnetic microcarriers and addresses the universal need of process control for synthesis in microfluidic networks, i.e., on-demand creation of droplet templates for high information capacity. The demonstration of magnetic suspension array technology enabled by magnetic in-flow cytometry opens the avenue toward point-of-care multiplexed bead-based assays, clinical diagnostics, and drug discovery.

1. Introduction

Information tags are ubiquitous in modern information-intensive society. The tags allow indexing, encryption, and identification of distinct types of information carriers, making them vital components in telecommunication,[1] forensic labeling,[2] anti-counterfeiting,[3] and biological screening.[4] Large-scale screenings in studies of gene expression,[5] combinatorial chemistries,[6] and small compound identification[7,8] entail information tags with indexing capacity ranging from thousands to millions. There are typically two formats for large-scale screening applications: planar microarrays[9] and suspension arrays.[10] Suspension array technology utilizes encoded microcarriers as information tags to associate distinct measurable signals with different variants in solutions. The technology allows the throughput of screening to be boosted by multiplexing and has proven its superior performance in terms of fast reactions kinetics, better probe binding, and flexibility of probe combinations.[11] Spectroscopic microparticles encapsulating, e.g., fluorescent dyes, has been practically and commercially applied,[12] as multiple colors of well-separated spectroscopic wavelengths allow 100% discrimination capability. Moreover, these encoded microparticles can be decoded by commercial flow cytometers at high throughput.[13] However, due to spectral overlap, commercial flow cytometers are limited to fewer than 20 channels but require expensive cumbersome components such as three to five lasers, tens

G. Lin, D. D. Karnaushenko, Prof. O. G. Schmidt, Dr. D. Makarov
Institute for Integrative Nanosciences
IFW Dresden
Helmholtzstr. 20, 01069 Dresden, Germany
E-mail: lingungun@gmail.com; d.makarov@hzdr.de
G. S. Cañón Bermúdez, Dr. D. Makarov
Helmholtz-Zentrum Dresden-Rossendorf e.V.
Institute of Ion Beam Physics and Materials Research
Bautzner Landstraße 400, 01328 Dresden, Germany

DOI: 10.1002/smll.201601166

of filters, and up to 20 detectors when multiple colors are involved.[14,15] More recent innovative graphical particles with codes embedded spatially in the microcarriers offer virtually unlimited encoding capacity,[16–18] but the start–stop code creation requires new sets of photomasks for each code. Due to the visual identification nature, instant feedback control continues to be challenging for applications where automated continuous-flow operations are needed.[19,20] On-demand creation and on-the-fly decoding of encoded microcarriers by a cost-effective and automated compact system remains to be a common pursue.

Substantial efforts have been devoted toward seeking for new encoding material and strategies to expand the encoding capability.[21,22] In this respect, the same requirement of high distinguishability, the ease of code generation, and the feasibility of fast code readout should be imposed to all alternative methods relying on other physical properties such as the amounts of encoding material and the size of encoding particles.[23] Magnetic materials hold promise to provide intrinsic advantages to suspension array technology that primarily relies on optics.[24] Spatially distributed magnetic stray fields exhibited by magnetic entities, when properly designed, may serve as distinct signals for encoding, which will not interfere with optical reporters. The instant perceptible feature of magnetic stray fields by a magnetic field sensor may further enable fast code readout. Magnetic materials have been mainly explored in terms of bringing an additional degree of freedom for manipulation of suspension arrays, which has proven to be efficient to enhance the reaction kinetics and facilitate code handling.[17,25] Nevertheless, the development of magnetic suspension array technology based on well-distinguishable magnetic encoding information is still hampered by the lack of direct access to the magnetic content during code preparation, and hence the lack of quality control and the ability to screen over the properties of individual magnetic entities. In this respect, smart systems are needed to direct decisions and impart quality administration and screening over the properties of individual encoded microparticles.

Here, we realize a smart and compact system for high degree of quality control for synthesis of encoded microparticles. With embedded droplet microfluidic networks, the system addresses the pressing need of controllably synthesizing magnetic suspension arrays ensuring 100% success rate of discrimination. The deterministic control over individual entities that is not feasible with existing batch synthesis methods in bulk solutions[26] represents the first approach to controlling the quality of encoded magnetic microcarriers. The approach of creating magnetic suspension arrays is mask-free which is different from existing approaches to fabricating graphical codes and allows automated continuous-flow operations. Furthermore, we show that the versatile system enables to deterministically assemble encoded droplet templates on demand, which is promising for synthesis of position-indexed suspension arrays of high capacity in microfluidic networks. The in-flow micro-magnetofluidic system is demonstrated as a unique and compact flow cytometric screening device allowing the analysis and discrimination of different batches of magnetic suspension arrays that can be potentially conjugated with ligands for multiplexed point-of-care bead-based assays.

2. Results and Discussions

2.1. Magnetic Suspension Array Technology: Concept and System Design

Our concept of magnetic suspension array technology is based on encapsulating distinct amounts of magnetic coding materials into single microcarriers to produce identifiable magnetic stray field patterns with a developed magnetic flow cytometric platform. However, conventional bulk synthesis approaches[26,27] to obtain well-identifiable magnetic field patterns are challenged by the incapability to control over the properties of individual entities, e.g., the amounts of magnetic content and the size of encoded microcarriers which determine whether well-identifiable magnetic stray field patterns can be produced. In this respect, droplet microfluidics offers an efficient format to impart control over the entities to be synthesized,[28–32] as this format allows reagents to be encapsulated into discrete droplet containers separately by an immobile oil phase and individual droplet containers can be interrogated. Our prior results showed that magnetic stray field patterns of droplets encapsulating magnetic nanoparticles evolve with the change of droplet contents and sizes,[33,34] which may serve as unique features of droplet containers when they are used as "templates" for synthesis of encoded magnetic microcarriers.

Magnetic field sensors exhibiting giant magnetoresistive (GMR) effect[35,36] are chosen as the detectors of the magnetic in-flow cytometric system to locally access, analyze, and select the properties of magnetic droplets in microfluidic networks into different batches of distinct properties as suspension arrays (**Figure 1**a). To be noted, this type of magnetic field sensors when patterned into micrometer size (compatible to the objects to be detected) response sensitively to the local variation of magnetic stray fields that may result from the change of the magnetic content and the volume of the droplets down to picoliters.[33] The detected peak pattern as featured by local signal maxima and minima reflects the characteristic local maxima and minima of magnetic stray fields of the droplets concentrated at the ends.[37,38] Thereby, the essence of our concept of magnetic suspension arrays technology lies in reliably creating and identifying magnetic stray field patterns that can be characterized by well-distinguishable detection peak patterns with a magnetic field sensor. In the spirit of optical flow cytometers for fluorescent-activated sorting, we equip our system with a magnetic-activated sorting function by integrating mechanical membrane valves[39] in microfluidic networks (details are provided in the Experimental Section and Figure S1, Supporting Information). When actuated and triggered by the detection signal of the magnetic field sensor, the membrane of the polydimethylsiloxane (PDMS) can be deflected by compressed air to close the bottom flow channel so that to the flow trajectory is changed due to the alteration of flow resistance. In this way, droplet templates can be isolated for further processing based on their interrogated properties.

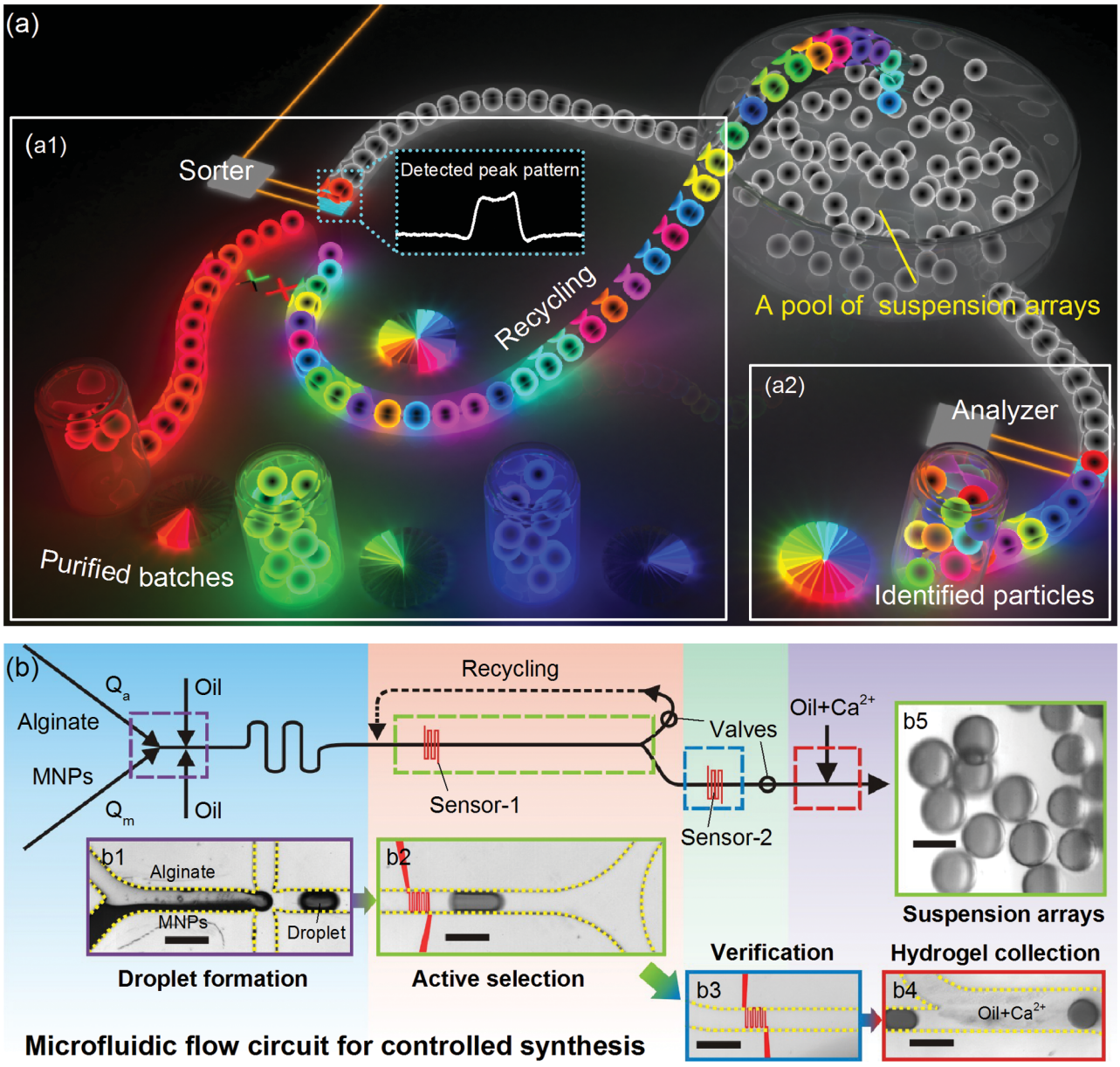

Figure 1. a) Conceptual image illustrating magnetic suspension array technology enabled by a magnetic flow cytometric system for controlled selection (a1) and identification (a2) of magnetic suspension arrays. A pool of magnetic microcarriers of unknown properties can be selected out (a1) into different batches based on analyzing the detection peak pattern corresponding to a selected property, e.g., magnetic content and size, which are identified by an implemented magnetic in-flow detector (a2). Each isolated batch is distinct from the others in terms of the selected property, which is analogous to fluorescent "color" coding. b) Rationally designed microfluidic flow circuit for the synthesis of magnetic hydrogel suspension arrays in the system equipped with an active selection functionality. Q_a and Q_m are the flow rates of alginate solution and magnetic nanoparticles (MNPs), respectively. b1–b4) Micrographs corresponding to the regions enclosed by dashed squares in the schematic flow circuit. b1) Micrograph of the droplet formation module where alginate solution and MNPs are coencapsulated in droplets with a hydrodynamic focusing design. b2,b3) Micrographs of an integrated magnetic sensor (sensor-1) for active selection of droplets into the designed channel where a second sensor is integrated downstream (sensor-2) for verification. b4) Gelation zone where oil with Ca^{2+} is injected from the top side channel. b5) Collected magnetic hydrogels at the system output. Scale bar: (b1–b4) 200 μm; (b5) 100 μm.

2.2. Controlled Synthesis of Magnetic Suspension Arrays

By integrating the system with conditioning circuits, the system offers the capability of active control over individual droplets via logic selection (details are provided in the Experimental Section). It hence allows us to perform deterministic operations over individual entities for controlled synthesis in microfluidic flow networks. With rationally designed microfluidic networks (Figure 1b), we demonstrate controlled synthesis and quality administration over the properties of encoded magnetic microparticles enabling for suspension array technology. For this particular purpose, we chose alginate hydrogel as the matrix of magnetic suspension arrays. To synthesize magnetic hydrogel-based suspension arrays, Ca^{2+} ions are used to crosslink the guluronic acid blocks of neighboring polymer chains of alginate via interactions with carboxylic groups

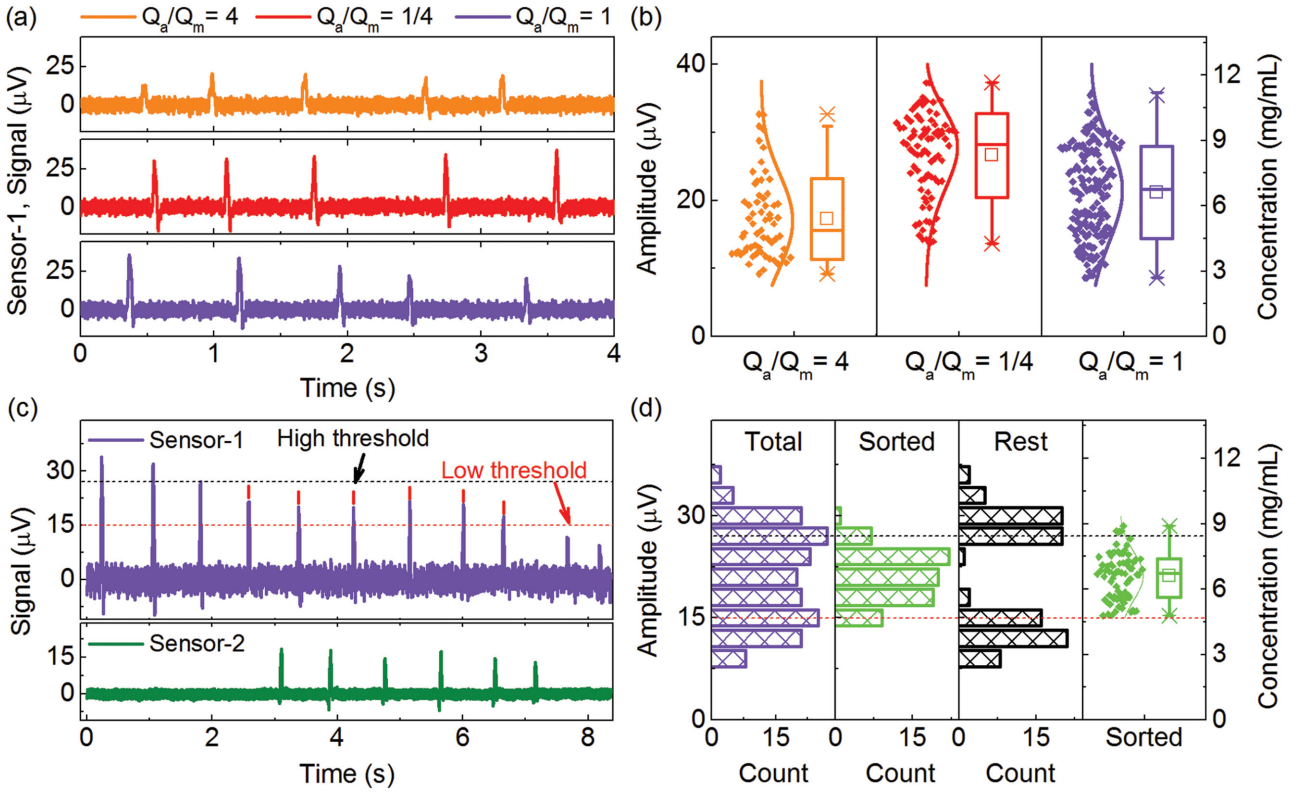

Figure 2. a) Real-time monitoring of the magnetic content of alginate droplets by flow regulation, i.e., changing different flow ratios of alginate and magnetic nanoparticles. Here, Q_a is the flow rate of alginate solutions and Q_m is the flow rate of magnetic nanoparticles. b) Distribution of the detected signal amplitude for different batches of droplets produced with different flow parameters. Here Q_a and Q_m is the same as in (a). The signal amplitude is extracted from the detection peaks in (a). The right vertical axis is the corresponding concentration of magnetic nanoparticles calibrated against the detected voltage signals. Each data set is presented as a scatter and a Tukey box plot (the box frames the data with standard deviations; the line shows the median; the square, the mean value; and the whiskers are the upper and lower fence of the data). c) Real-time detection data of a train of alginate droplets carrying various amounts of magnetic content by sensor-1 as shown in Figure 1b. A high and a low threshold voltage are defined to actively select a batch of droplets with detected voltage signal amplitude falling in between the high and low threshold values. The bottom panel shows the detected signals of the sensor-2. Vertical bars above the detection peaks indicate the droplets that are actually sorted out. d) Distribution of the detected signal amplitude and corresponding concentrations of magnetic content of the whole batch of droplets, the sorted batch, and the rest (unsorted). The horizontal dashed lines are the high and low selection thresholds as in (c).

in the sugars to form the gel networks.[40] We encapsulate first superparamagnetic nanoparticles and alginate solutions in droplets by a flow focusing geometry[41] and employ an internal flow recirculation mechanism in droplet microfluidics to mix the two components (Figure 1(b1)). Ferrofluid superparamagnetic nanoparticles of magnetic cores less than 50 nm do not retain magnetic moment without applying an external magnetic field. Hence, there is no agglutination issue typically arising from magnetic dipolar interaction and thus facilitating the quantification and reproducibility of the magnetic content loaded in a single-droplet template. Moreover, unlike conventional bulk synthesis methods,[26] the active droplet selection module with an integrated magnetic field sensor (Figure 1(b2), sensor-1) in the flow circuit enables to select droplets based on the signal readout of the sensor into a desired output channel, where Ca^{2+} ions are introduced from a side channel right after the second magnetic field sensor (Figure 1(b3), sensor-2) to fully crosslink the alginate matrix near the exit of the microfluidic flow circuit (Figure 1(b4)). With this rationally designed route, all magnetic microgels are produced of desired regular spherical shapes (Figure 1(b5) and Figure S2, Supporting Information). Such a flow circuit design avoids the typical operations of droplet reactors for synthesis. For instance, the co-injection of all components such as magnetic particles, alginate, and Ca^{2+} in the droplet containers is most likely to result in an uncontrolled irregular shape of hydrogels with only about 34% loaded with homogenous content (Table S1, Supporting Information).

To demonstrate the direct access to the magnetic content of the microgels during synthesis, we change the flow ratio of the two components of magnetic nanoparticles and alginate solutions. With distinct flow ratios, different batches of alginate droplets can be produced with different dominant concentrations of encapsulated magnetic particles. These produced magnetic alginate droplets are detected by the sensor-1, as the real-time data are featured with isolated detection peaks (**Figure 2**a). Hence, the scattered signal amplitude reflects a deviation in the distribution of encapsulated magnetic particles while the varied median/mean values of the scattered plots evidence the variations of the dominant concentrations of encapsulated magnetic content produced by different flow parameters[42] (Figure 2b). This provides information on the magnetic properties and their distribution in a batch. This quantitative information was not accessible

before, though closely relevant to produce magnetic suspension arrays. The result also suggests that despite the intrinsic advantages of droplet microfluidics for synthesis based on emulsion templates, deviations of the encapsulated content possibly arising from flow instability, tubing connections, and pumps should be practically considered. However, by introducing the quality control stage in the system, we can perform active selection (gating) of the alginate droplets which are subsequently cross-linked into microgels and assigned into a single batch as a type of magnetic suspension arrays. In this case, the distribution of magnetic properties from bead to bead in a batch can be determined while forming a batch. This feature is crucial to predefine the properties of suspension arrays utilized for encoding which can be eventually applied for flow cytometric screening.

Apart from the direct access to the magnetic properties of droplet templates, the signal of the sensor-1 can be used to switch the flow. For instance, a batch of droplet templates with the detection signals falling in between two predefined high and low threshold voltages is selected out of the initial train of droplets detected by the sensor-1, as verified by the signals detected by the sensor-2 (Figure 2c). Thereby, as shown, we are capable of actively gating a population of droplets of a wider deviation in the magnetic content into a batch with about threefold improvement in the deviation of the magnetic content (Figure 2d). The narrowest range of voltage signals the system can distinguish is determined by how much the voltage signal of a droplet is different from an applied threshold value, within which the system cannot differentiate and thus successfully sort out the droplet. As shown in Figure 2d, for both threshold values applied, one can observe that the sensitivity of the system in differentiating voltage signals is 3 μV, which results in the fact that droplets with voltage signals, that is, within 3 μV different from an applied threshold value cannot be successfully sorted out. With the precision of the magnetic field sensor in differentiating voltage signal difference down to 3 μV, the precision of the system in isolating droplet templates of various concentrations of encapsulated magnetic content is estimated down to about 1 mg mL^{-1}. The precision enables the system to practically produce magnetic suspension arrays based on most commercially available ferrofluid superparamagnetic nanoparticles, e.g., EMG series (Ferrotec), fluidMAG (ChemiCell) with stock concentrations up to a few tens of mg mL^{-1}.

2.3. Magnetic In-Flow Cytometry

One of the crucial aspects to practically apply suspension array technology for high-throughput screening is that the encoded microcarriers need to be well identified on the fly. Different batches of purified magnetic hydrogels represent different types of encoded microcarriers, in this respect, providing distinct magnetic signals, which is analogous to optically encoded microparticles exhibiting distinct colors. The encoded magnetic microcarriers can be purified and identified into different batches (analogous to optical colored codes) by the developed magnetic flow cytometric system with an integrated magnetic detector. To demonstrate the flow cytometric screening of different batches of encoded microcarriers, we apply a standard flow cytometric analysis method based on the size and the concentration of encapsulated magnetic content of different batches of magnetic alginate droplet templates which are physically purified and isolated by our selection module prior to their gelation. To compare the distinguishability of different batches produced, we apply a supervised discriminant analysis technique[43] to allocate the detection events (scattered points) from two different batches of particles into each other. The probability of a detection event belonging to its original batch is illustrated with a color map (algorithm is provided in the Experimental Section). For comparison, with two sets of distinct flow rate ratio (typical to load distinct amounts of species in droplets) but without active selection, it is found that the detection of the two batches of as-produced droplet templates shows a large signal overlap, leading to a large rate of misallocation of 22% (**Figure 3**a,b). This result points out the importance to implement the quality control module for synthesis of suspension arrays. By active selection, two batches of droplets produced by one set of flow parameters isolated by the same threshold voltage (zero confidence margin, Figure 3c(1,2)) already show a reduced error rate of discrimination about 8% (Figure 3d(1)). To further increase the discrimination capability, another batch of droplet templates is selected at a different threshold voltage well separated from the initial one (nonzero confidence margin, Figure 3c(3,4)). Hence, 100% of discrimination efficiency can be achieved, i.e., between batches A and C (Figure 3d(2)). Such multiple selections of magnetic alginate droplet templates with quality control enable the system to deterministically produce well-distinguishable encoded suspension arrays.

The number of channels for a magnetic system is determined (i) by the number of distinct parameters, which can be used to extract distinguishable encoding information and (ii) by the detection limit of the sensing platform. As is shown that the detected signal peak width is proportional to the size of the droplets[37,38] (Figure S3, Supporting Information), the system can be extended to select magnetic alginate droplet templates of different sizes by defining a threshold peak width for selection into different batches (details are provided in the Experimental Section). The system is capable of isolating droplets with tolerance down to 2 μm with a high sorting fidelity (**Table 1**). This result opens up the possibility to encode microparticles which may rely not only on the channel of loaded magnetic content but also on other channels (physical parameters), e.g., the size, and thus boosting the encoding capability.

2.4. Deterministic Formation of Encoded Droplet Templates toward High Information Capacity

Toward high information capacity, Zhao et al.[44–46] reported an innovative approach for synthesis of high-capacity codes based on photonic crystals and quantum dots with double-emulsion templates in droplet microfluidics. These templates are subsequently solidified into single entities as suspension arrays. The existing approach relies on

www.MaterialsViews.com

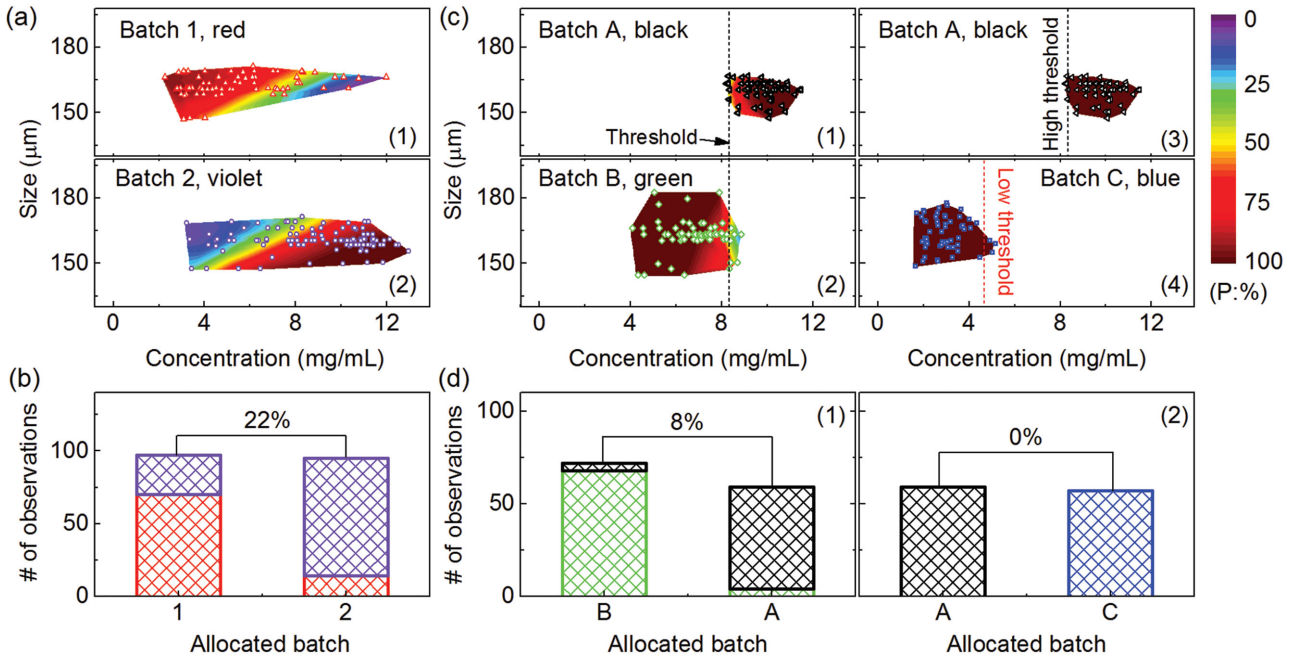

Figure 3. a) Multiparametric scatter plot of two batches of magnetic droplet templates characterized by their size and concentration of encapsulated magnetic content. The two batches of droplets are produced by two distinct flow ratios of alginate and magnetic nanoparticles without active selection: a1) $Q_a/Q_m = 4$ and (a2) $Q_a/Q_m = 1/4$. Each point indicates a detection event of a droplet. The color map shows the probability (P) of a detection event belonging to the original batch evaluated by a statistical algorithm (details are given in the Experimental Section). b) Discrimination result of the mutual allocation of the detection events between two batches of magnetic alginate droplets (batches 1 and 2 as in (a)) without active selection. The height of the bar shows the number of the detection events and the color indicates the batch the detection events originally belong to. The number 22% indicates the total error rate of discrimination. c) Multiparametric scatter plots of different batches of droplets produced by active selection. c1–c4) Batches A and B are selected out with the same threshold voltage (zero confidence margin) as indicated by the black dashed line. Batch C is selected out by setting a lower threshold voltage (red dashed line) further apart from the higher threshold voltage (nonzero confidence margin). d) Discrimination result of allocating the detection events between two batches of droplets (batches A and B or batches A and C) produced by active selection. The numbers 8% and 0% indicate the total error rates of the discrimination.

hydrodynamic-focusing shear flows to encapsulate elementary droplets into templates, but it is not yet feasible to arrange each elementary droplet to form unique sequences "on demand." For simplicity, binary droplet templates can be embodied by a train of spatially arranged elementary droplets encapsulating distinct amounts of magnetic material providing two distinct high and low levels of detection signals as elementary logic bits "1" and "0," respectively (**Figure 4**a,b). The formulation of logic bits "1," and "0," relies on the creativon of two clear distributions of detected signal levels falling in two confined regions separated with a confidence margin to ensure precise differentiation of the binary states (Figure 4c,d). However, by using two T-junctions to passively produce two types of droplets consisting of different concentrations of magnetic nanoparticles via continuous fluidic pumping and flow regulations, the formation of the droplets is prone to establish an equilibrium state, i.e., regular sequences consisting of alternating droplets. This indicates that without introducing an active selection function, it is most likely to form one type of droplet templates without switching the process (e.g., exchanging the types of elementary droplets or flow conditions).

Under such circumstances, we propose an alternative approach by using the selection system to accomplish the task. By defining a selection threshold falling in between the confidence regions, individual elementary droplets are actively selected by the system out of a master sequence. In this way, unique encoding droplet templates can be formulated by virtually any combination of elementary droplet bits of predefined length. Starting from a master sequence, without switching the process it is feasible to realize droplet templates of any complexity and length in continuous flow with the active droplet selection system. For instance, a series of droplet templates composed of four elementary droplets representing "0001," "0010," "0011," and "0100" which correspond to decimal numbers "1," "2," "3," and "4" are generated consecutively on demand (Figure 4e). This demonstrates that meaningful encoding information can be stored inside the sequences. Such position-indexed sequences bear potential to boost the encoding capacity of suspension arrays, as the total multiplexing capacity grows substantially with the number

Table 1. Size-based sorting.

Tolerance[a] [μm]	Beyond tolerance		Within tolerance		Fidelity[b] [%]
	OUT A	OUT B	OUT A	OUT B	
2	7	2	196	138	97
4	3	1	200	139	99

[a]The definition of the tolerance is provided in Supporting Information, Figure S3; [b]The sorting fidelity is evaluated by the number of droplets within the tolerance over the total number of droplets sorted.

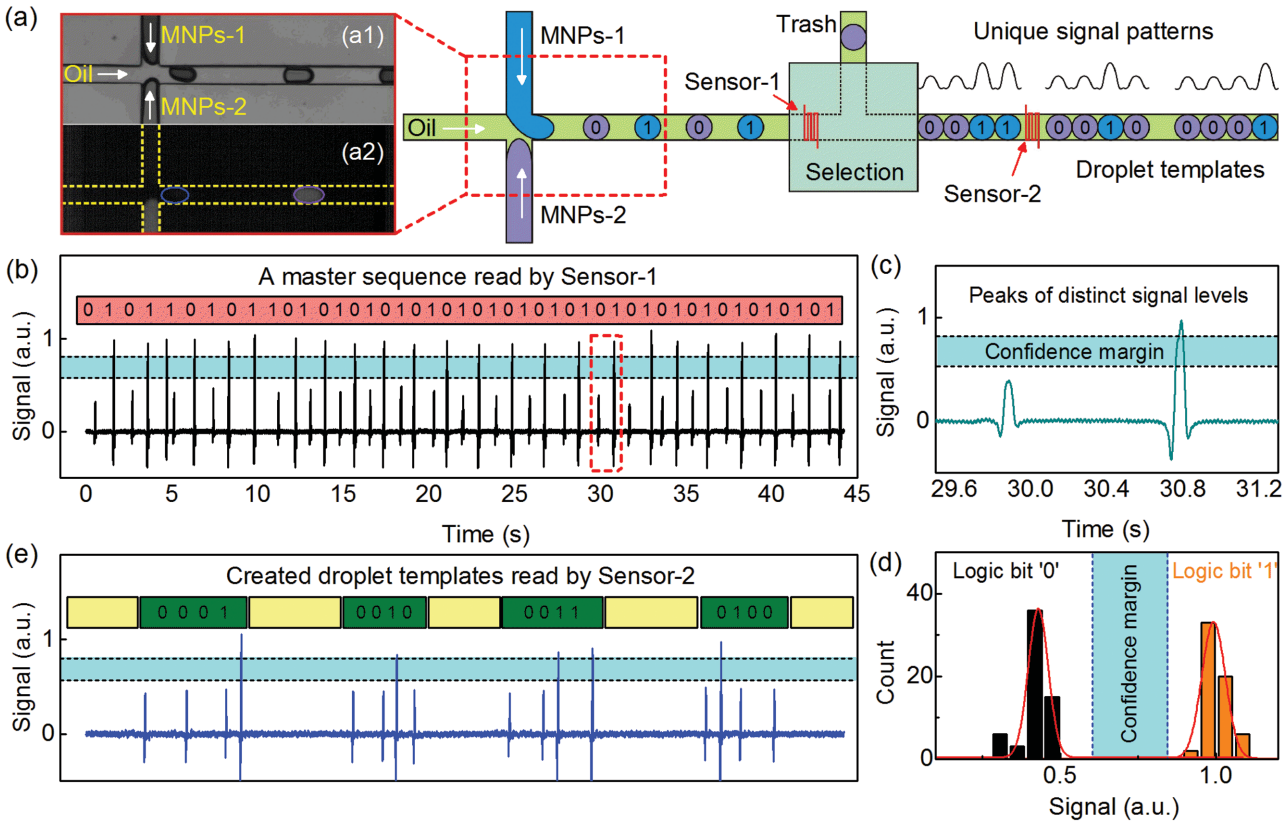

Figure 4. a) Schematic sketch of a microfluidic flow circuit with an implemented active selection module for on-demand creation of droplet templates for high information capacity. Binary droplets loaded with high and low concentrations of magnetic nanoparticles (MNPs-1 and MNPs-2) are produced by hydrodynamic shear flows with two confronting T-junctions. The as-formed master droplet sequences are read by the sensor-1 which controls the selection module to actively create desired droplet templates for encoding. The created droplet templates are read and verified by the sensor-2 integrated downstream. a1,a2) Bright-field and fluorescence micrographs of the binary droplets formation geometry. Droplets are co-loaded with fluorescent dyes for visualization. High-concentration MNPs are loaded with low-concentration fluorescent dyes thus giving low contrast, and vice versa. b) The master droplet sequence and created droplet templates read by the sensor-1 (top) and the sensor-2 ((e), bottom), respectively. The droplet templates are created on the fly which correspond to the decimal integer number from 1 to 4. c) The magnified area of the data as indicated by a red dashed square in (b). The dashed regions show the confidence regions with the edges defined by the 95% confidence levels of the distribution of the two distinct signal levels as shown in (d). The high and low levels of signals are defined as logic "1" and "0," respectively.

of distinguishable signal levels (m) and the length (N) of the templates, which is given by $(m^N+m)/2$ (here the factor of 1/2 is used due to the inverse symmetry of the templates, for instance, "0001" is considered identical to "1000" in suspension, while original symmetric template sequences such as "1001" and "0110" do not need to consider this effect). The number of signal levels (m) is ultimately determined by the dynamic range and the resolution of the magnetic field sensor in selection. With the present stock concentration of magnetic nanoparticles (EMG 700 series, 75 mg mL^{-1}) and the resolution of the sensor (1 mg mL^{-1}), the maximum number of distinguishable signal levels that can be created by selection is estimated to be in the order of 70 (without adding the dimensionality of size-based encoding). This may require the length of the droplet templates to be at least 4 in order to reach an information capacity exceeding 10^6 as generally needed for drug discovery applications. To be noted, by properly choosing the crosslinking agents and fluidic methods, to encapsulate droplet templates consisting of four elementary droplets into single entities has been practically proven feasible by Zhao et al.[44,46]

The application of the system to deterministically create batches of well-distinguishable magnetically encoded microcarriers and screening with a magnetic flow cytometric platform offers the first solution to create nonoptically encoded microcarriers as an analog of multiple optical "colors" for commercial suspension array technology. Such encoded microcarriers do not interference with fluorescent reporters in multiplexed bioassays and diagnostics and expand the encoding capability of existing methods.[22] The present elementary droplet templates for synthesis are of sizes in the order of 100 μm, a common scale for microfluidic systems. However, the size of the templates could be downscaled and adapted to new systems with smaller channel geometries together with the size of magnetic field sensors to simplify the existing optical systems with less filters and light sources. Such scalability could be relevant for synthesizing encoded particles for suspension array technology where the particles with sizes of a few tens of micrometers are of considerable interest.[23]

3. Conclusion

We demonstrate a magnetic flow cytometric system for controlled synthesis and screening of magnetic suspension arrays in microfluidic networks. The system provides an important approach for the emerging suspension arrays technologies[22] in terms of the ease and flexibility of code creation, the capability of continuous-flow decoding with a compact cost-effective flow cytometric system and the potential to achieve high information capacity. The device allows us to directly access and control the properties of individual magnetic microcarriers during synthesis, which offers the very first solution for the quality administration of magnetic suspension arrays. The capability to deterministically create unique droplet sequences as encoding templates holds promise to realize high-capacity magnetic suspension arrays. Controlled synthesis of magnetic suspension arrays with high precision in microfluidic networks starting from tiny amounts of magnetic nanomaterials could bring perspectives for industrial applications, for which the system provides a seamless connection to magnetic bead manufacturers. With high degree of process control and complete functionalities we further anticipate that it will ultimately allow researchers and clinicians to run large-scale biological screening in microfluidic networks with full automation.

4. Experimental Section

Fabrication of the Microfluidic System: A silicon wafer with 600 nm natural oxides was patterned by standard photolithography steps with a photoresist AZ5214 E and a mask aligner (Karl Suss MJB4) to define the geometry of the sensor with a meander shape consisting of nine turns of stripes (length: 100 µm; width: 6 µm). The GMR stack consisting of [Py (1.6 nm)/Cu (2.3 nm)]$_{30}$ was deposited by magnetron sputter deposition with base pressure $<10^{-6}$ mbar on the patterned substrate. Deposition parameters are the following: Ar as the sputter gas, sputter pressure 9.5×10^{-4} mbar and flow rate 10 sccm. After lift-off, a layer of photoresist SU-8 2 of about 700 nm was coated on the GMR sensor chip for electrical insulation. The resist was baked and exposed by ultraviolet light to be ready for bonding.

The microfluidic channel was made by casting PDMS polymer in an SU-8 mold. The mold was fabricated by a UV lithographic technique with a photoresist SU-8 50 of 65 µm and its geometry was created by a microwriter (MicroWriter MLBaby, Durham Magneto Optics Ltd.) with a power density of 700 mJ cm^{-2}. The PDMS prepolymer (Sylgard 184, Dow Corning) was prepared by mixing a base polymer with a cross-linking agent. The main flow channels were fabricated by coating the PDMS prepolymer on a mold at a speed of 1500 rpm for 30 s, which was cured at 120 °C for 1 min. The control channels were fabricated with a second SU-8 50 mold. The cured control channels and flow channels were bonded to each other after activation with O_2 plasma and baked at 120 °C for 5 min to create a PDMS cap. To assemble the final device, the PDMS cap was activated in N_2 plasma (40 mW) to create amine-terminated surface. The GMR sensor chip insulated with the resist of SU-8 2 was attached to the PDMS cap under a microscope while the permanent bonding was achieved by baking at 120 °C for 20 min.

Formation of Magnetic Droplets: To form binary droplet bits, magnetic superparamagnetic particles (Chemicell GmbH, stock concentration: 25 mg mL^{-1}) diluted into 15 mg mL^{-1} and 5 mg mL^{-1} were used as the disperse phase, and mineral oil (Sigma-Aldrich, M8510) with 5% SPAN 80 was used as the continuous phase. The fluids were loaded in separate syringes and pumped to the microfluidic device through polytetrafluoroethylene (PTFE) tubes (OD: 0.9 mm; ID: 0.4 mm). Syringe pumps (Cetoni GmbH, neMESYS) were used to control the flow parameters.

Microfluidic Measurements and Operations: For real-time signal acquisition, the GMR sensor was included as a component of a Wheatstone bridge (Figure S4, Supporting Information). A lock-in amplifier (Stanford Research Systems, SR830) powered the circuit with an AC driving current of 1 mA. The differential voltage of the bridge was picked up by the lock-in amplifier to amplify the signal and reduce the noise. The modulation frequency was set to 1 kHz, and the analog output of the processed signal was fed into a data acquisition box (DAQ, NI-USB 6009). A permanent magnet (AlNiCo 500, type A1560, IBSMagnet, length: 60 mm, diameter: 15 mm) was used to bias the sensor to the most sensitive region and used to simultaneously magnetize the magnetic nanoparticles. The position of the magnet was adjusted carefully to obtain an optimum signal output while pumping droplets across the sensor.

For active selection of droplets, the microfluidic membrane valves were connected with a 3-way isolation valve (Cetoni GmbH, one way open, one way closed) via PTFE tubes through which pressurized gas was applied to control the membrane valves. A LabVIEW control program and a control circuit were designed and constructed for the magnetically activated selection. The voltage signal from the DAQ was computed in the LabVIEW program to evaluate the voltage change in real time by detecting the rising edge. The total voltage change (the signal amplitude) with respect to the background was compared with a base threshold voltage value that defines a droplet detection event. For active selection, the voltage signal amplitude of a detected droplet was further compared with a second threshold selection voltage, the result of which determines the logic state "1" and "0" and were computed with the instruction control to generate the logic output. An instruction input was applied to control the length of the droplet templates and cluster arrays to store binary digital values of "1" and "0" were programed to create a droplet template with desired sequence and length. For the quality control for particle synthesis, a selection range is defined by different threshold voltages to actively actuate the valves. Alternatively, for characterization of the size-based selection, the detection peak width has been used as a sorting criterion, the algorithm of extracting the peak width has been described elsewhere.[47] In brief, the peak width is determined by the temporal shift between the rising and falling edges of the detection peak. And the rising and falling edges are determined by detecting the maximum of the squared second derivative of the voltage signal. The rate of the selection is determined by the switching time of the used mechanical valves (about 40 ms).

Synthesis of Magnetic Hydrogel Particles: The alginate solution was prepared by dissolving sodium alginate powders (Sigma-Aldrich GmbH) in deionized (DI) water at a ratio of 1 wt% and filtering away remaining precipitates. To prepare the Ca^{2+} bath to crosslink alginate droplets[51], 1 g of calcium chloride (Sigma-Aldrich GmbH) was

mixed first with 10 mL 2-methyl-1-propanol (Sigma-Aldrich GmbH) by ultrasonication for 5 h at 70 °C. Next, the solution was mixed with 10 mL oleic acid (Fisher Scientific GmbH). The whole solution was placed on a hotplate at 100 °C overnight to distill away the solvent of 2-methyl-1-propanol. The distilled solution was filtered to remove precipitates for use. For the formation of magnetic alginate droplets, magnetic particles (Chemicell GmbH) and the prepared alginate solution were brought into a microfluidic channel as the disperse phase. Oleic acid was used as the continuous phase. The magnetic alginate droplets were passed through the gelation zone to form hydrogel particles where the solution containing Ca^{2+} and oleic acid were injected from a side channel.

Algorithm of Supervised Discriminant Analysis: The analysis was conducted by calculating the within-group covariance matrix of each group to evaluate the Mahalanobis distance between each detection event within the droplet group. The posterior probability of a detection event allocated to a specific group was evaluated based on the group's covariance matrix and the Mahalanobis distance of the detection event from the group. The posterior probability of a detection event was computed for every droplet group and the detection event was allocated to the group which provides the largest posterior probability.

The within-group covariance matrix of a droplet group k is defined as[47]

$$\sum_k = \begin{bmatrix} \Sigma_{11} & \Sigma_{12} \\ \Sigma_{21} & \Sigma_{22} \end{bmatrix} = \begin{bmatrix} E\left[(X_i-\overline{X}_i)(X_i-\overline{X}_i)\right] & E\left[(X_i-\overline{X}_i)(X_j-\overline{X}_j)\right] \\ E\left[(X_j-\overline{X}_j)(X_i-\overline{X}_i)\right] & E\left[(X_j-\overline{X}_j)(X_j-\overline{X}_j)\right] \end{bmatrix} \quad (1)$$

Here, Σ_{ij} (i, j = 1, 2) is the covariance of the ith-variable x_i and jth-variable x_j, and $E(x_i, x_j)$ is the expectation of the product of variables x_i and x_j, and the mean values of the variable x_i and x_j in the droplet group, respectively. In this study, the variables x_i and x_j are the signal amplitude and the peak width obtained from the detection peaks.

The Mahalanobis distance D_{X_k} measures the distance of a detection event of a droplet $X = (x_i, x_j)$ from the detection events in a droplet group k. It is given by[48]

$$D_{X_k} = \sqrt{(X-\overline{X_k})^T \Sigma_k^{-1} (X-\overline{X_k})} \quad (2)$$

with $\overline{X_k}$ being the mean value of the distribution of the droplet events in the droplet group k, and Σ_k^{-1} the inverse of the covariance matrix of the group k.

The posterior probability of a detected event X belonging to a droplet group k is computed by the following equation[49]

$$\log(qxk) = -\frac{1}{2} D{x_k}^2 + \log(\pi_k) - \frac{1}{2}\log\left|\sum_k\right| + c_0 \quad (3)$$

Here, c_0 is used to normalize the posterior probability of all detection events.

Supporting Information

Supporting Information is available from the Wiley Online Library or from the author.

Acknowledgements

The authors thank Dr. Mariana Medina (IFW Dresden) for fruitful discussion and Irina Fiering (IFW Dresden) for sputter deposition of metals. The work was financially supported in part by the DFG Research Group 1713 and the European Research Council under the European Union's Seventh Framework Programme (FP7/2007-2013)/ERC Grant Agreement No. 306277.

[1] F. D. Smith, F. H. Campos, K. Jeffay, D. Ott, *ACM SIGMETRICS Perform. Eval. Rev.* **2001**, *29*, 245.
[2] J. D. Livingston, K. R. Rossiter, S. N. Verdun-Jones, *Psychiatry Res.* **2011**, *188*, 115.
[3] S. Han, H. J. Bae, J. Kim, S. Shin, S.-E. Choi, S. H. Lee, S. Kwon, W. Park, *Adv. Mater.* **2012**, *24*, 5924.
[4] F. Cunin, T. A. Schmedake, J. R. Link, Y. Y. Li, J. Koh, S. N. Bhatia, M. J. Sailor, *Nat. Mater.* **2002**, *1*, 39.
[5] A. R. Abate, T. Hung, R. A. Sperling, P. Mary, A. Rotem, J. J. Agresti, M. A. Weiner, D. A. Weitz, *Lab Chip* **2013**, *13*, 4864.
[6] I. Takeuchi, J. Lauterbach, M. Fasolka, *Mater. Today* **2005**, *8*, 18.
[7] A. Fedarovich, K. A. Djordjevic, S. M. Swanson, Y. K. Peterson, R. A. Nicholas, C. Davies, *PLoS One* **2012**, *7*, e44918.
[8] W. Wang, J. R. Walker, X. Wang, M. S. Tremblay, J. W. Lee, X. Wu, P. G. Schultz, *Proc. Natl. Acad. Sci. USA* **2009**, *106*, 1427.
[9] S. Pang, J. Smith, D. Onley, J. Reeve, M. Walker, C. Foy, *J. Immunol. Methods* **2005**, *302*, 1.
[10] J. P. Nolan, L. A. Sklar, *Trends Biotechnol.* **2002**, *20*, 9.
[11] S. Birtwell, H. Morgan, *Integr. Biol.* **2009**, *1*, 345.
[12] R. J. Fulton, R. L. McDade, P. L. Smith, L. J. Kienker, J. R. Kettman, *Clin. Chem.* **1997**, *43*, 1749.
[13] J. R. Kettman, T. Davies, D. Chandler, K. G. Oliver, R. J. Fulton, *Cytometry* **1998**, *33*, 234.
[14] Y. Lu, J. Zhao, R. Zhang, Y. Liu, D. Liu, E. M. Goldys, X. Yang, P. Xi, A. Sunna, J. Lu, Y. Shi, R. C. Leif, Y. Huo, J. Shen, J. A. Piper, J. P. Robinson, D. Jin, *Nat. Photonics* **2013**, *8*, 32.
[15] S. P. Perfetto, P. K. Chattopadhyay, M. Roederer, *Nat. Rev. Immunol.* **2004**, *4*, 648.
[16] J. Lee, P. W. Bisso, R. L. Srinivas, J. J. Kim, A. J. Swiston, P. S. Doyle, *Nat. Mater.* **2014**, *13*, 524.
[17] H. Lee, J. Kim, H. Kim, J. Kim, S. Kwon, *Nat. Mater.* **2010**, *9*, 745.
[18] D. C. Pregibon, M. Toner, P. S. Doyle, *Science* **2007**, *315*, 1393.
[19] S. R. Nicewarner-Pena, R. G. Freeman, B. D. Reiss, L. He, D. J. Pena, I. D. Walton, R. Cromer, C. D. Keating, M. J. Natan, *Science* **2001**, *294*, 137.
[20] K. Braeckmans, S. C. De Smedt, C. Roelant, M. Leblans, R. Pauwels, J. Demeester, *Nat. Mater.* **2003**, *2*, 169.
[21] Y. Lu, J. Lu, J. Zhao, J. Cusido, F. M. Raymo, J. Yuan, S. Yang, R. C. Leif, Y. Huo, J. A. Piper, J. Paul Robinson, E. M. Goldys, D. Jin, *Nat. Commun.* **2014**, *5*, 3741.
[22] Y. Leng, K. Sun, X. Chen, W. Li, *Chem. Soc. Rev.* **2015**, *44*, 5552.
[23] K. Braeckmans, S. C. De Smedt, M. Leblans, R. Pauwels, J. Demeester, *Nat. Rev. Drug Discovery* **2002**, *1*, 447.
[24] C. S. S. R. Kumar, *Magnetic Nanomaterials*Wiley-VCH, Weinheim, Germany **2009**.
[25] K. W. Bong, S. C. Chapin, P. S. Doyle, *Langmuir* **2010**, *26*, 8008.
[26] C. Ménager, O. Sandre, J. Mangili, V. Cabuil, *Polymer* **2004**, *45*, 2475.
[27] C. Echeverria, P. Soares, A. Robalo, L. Pereira, C. M. M. Novo, I. Ferreira, J. P. Borges, *Mater. Des.* **2015**, *86*, 745.
[28] S.-Y. Teh, R. Lin, L.-H. Hung, A. P. Lee, *Lab Chip* **2008**, *8*, 198.
[29] X. Casadevall i Solvas, A. deMello, *Chem. Commun.* **2011**, *47*, 1936.
[30] X.-H. Ji, W. Cheng, F. Guo, W. Liu, S.-S. Guo, Z.-K. He, X.-Z. Zhao, *Lab Chip* **2011**, *11*, 2561.

[31] H. Song, D. L. Chen, R. F. Ismagilov, *Angew. Chem. Int. Ed.* **2006**, *45*, 7336.
[32] D. K. Hwang, D. Dendukuri, P. S. Doyle, *Lab Chip* **2008**, *8*, 1640.
[33] G. Lin, D. Makarov, M. Melzer, W. Si, C. Yan, O. G. Schmidt, *Lab Chip* **2014**, *14*, 4050.
[34] G. Lin, L. Baraban, L. Han, D. Karnaushenko, D. Makarov, G. Cuniberti, O. G. Schmidt, *Sci. Rep.* **2013**, *3*, 2548.
[35] G. Binasch, P. Grünberg, F. Saurenbach, W. Zinn, *Phys. Rev. B* **1989**, *39*, 4828.
[36] M. Baibich, J. Broto, A. Fert, F. Van Dau, *Phys. Rev. Lett.* **1988**, *61*, 2472.
[37] G. Lin, D. Makarov, O. G. Schmidt, *Sensors* **2015**, *15*, 12526.
[38] N. Pekas, M. D. Porter, M. Tondra, A. Popple, A. Jander, *Appl. Phys. Lett.* **2004**, *85*, 4783.
[39] M. A. Unger, *Science* **2000**, *288*, 113.
[40] A. D. Augst, H. J. Kong, D. J. Mooney, *Macromol. Biosci.* **2006**, *6*, 623.
[41] S. L. Anna, N. Bontoux, H. A. Stone, *Appl. Phys. Lett.* **2003**, *82*, 364.
[42] G. Lin, D. Makarov, M. Medina-Sánchez, M. Guix, L. Baraban, G. Cuniberti, O. G. Schmidt, *Lab Chip* **2015**, *15*, 216.
[43] G. Lin, V. M. Fomin, D. Makarov, O. G. Schmidt, *Microfluid. Nanofluid.* **2015**, *19*, 457.
[44] Y. Zhao, H. C. Shum, H. Chen, L. L. A. Adams, Z. Gu, D. A. Weitz, *J. Am. Chem. Soc.* **2011**, *133*, 8790.
[45] Y. Zhao, Z. Xie, H. Gu, L. Jin, X. Zhao, B. Wang, Z. Gu, *NPG Asia Mater.* **2012**, *4*, e25.
[46] Y. Zhao, Y. Cheng, L. Shang, J. Wang, Z. Xie, Z. Gu, *Small* **2015**, *11*, 151.
[47] N. H. Timm, *Applied Multivariate Analysis*, Springer-Verlag, New York, **2002**.
[48] R. De Maesschalck, D. Jouan-Rimbaud, D. L. Massart, *Chemom. Intell. Lab. Syst.* **2000**, *50*, 1.
[49] Details on the calculation of the posterior probability, http://www.originlab.com/doc/Origin-Help/DiscAnalysis-Algorithm (accessed: June 2016).

Received: April 5, 2016
Revised: June 12, 2016
Published online: July 18, 2016